Renewable and Sustainable Energy Reviews 28 (2013) 812–823

Contents lists available at ScienceDirect

Renewable and Sustainable Energy Reviews

journal homepage: www.elsevier.com/locate/rser

Real-time analysis of low-concentration photovoltaic systems: A review towards development of sustainable energy technology

Pankaj Yadav [a], Brijesh Tripathi [a,b], Siddharth Rathod [a], Manoj Kumar [b,*]

[a] School of Solar Energy, Pandit Deendayal Petroleum University, Gandhinagar, Gujarat-382007, India
[b] School of Technology, Pandit Deendayal Petroleum University, Gandhinagar, Gujarat-382007, India

ARTICLE INFO

Article history:
Received 21 March 2013
Received in revised form
2 August 2013
Accepted 11 August 2013
Available online 8 September 2013

Keywords:
Low-concentration photovoltaic (LCPV) system
Dynamic resistance
Silicon solar PV module
LCPV power plant
Performance ratio

ABSTRACT

This article explores the potential of 1 kW_P low-concentration photovoltaic (LCPV) system for commercial purposes. Real-time analysis of in-house developed LCPV system shows better performance than the flat panel PV systems. Under actual test conditions (ATC), the open-circuit voltage (V_{OC}) decreases with temperature coefficient of voltage ≈ -0.061 V/K. The dynamic resistance is found to have a positive coefficient of module temperature i.e., $dr_d/dT \approx 0.49\ \Omega/K$. The annual energy generation of 1 kW_P LCPV power plant is envisaged as 1747.2 kW h/kW_P while the annual average daily final yield, reference yield and array yield were 3.76, 5.09 and 4.29 h/day, respectively. The annual average daily performance ratio and capacity factor are 72% and 14%, respectively. The annual average daily system losses and capture losses are 0.57 and 0.80 h/day correspondingly.

Contents

1. Introduction

In the last decade, solar energy has emerged as a promising resource of green energy alternative to non-renewable energy resources. Solar energy is probably the strongest-growing electricity generation technology, demonstrating recent annual growth rates of around 23% and worldwide production of 32.34 GW in 2012 consisting of both grid-connected and off-grid remote power supplies [1]. Besides playing noteworthy role in the future energy blend, PV generation is significantly contributing to the environmental impact of the electricity supply. PV technology is one of the best ways to harvest the solar energy since PV requires very little maintenance and is capable of giving output from microwatts to

* Corresponding author. Tel.: +91 79 2327 5328; fax: +91 79 2327 5030.
E-mail addresses: manoj.kumar@sse.pdpu.ac.in, manoj.kspv@gmail.com (M. Kumar).

1364-0321/$ - see front matter © 2013 Elsevier Ltd. All rights reserved.
http://dx.doi.org/10.1016/j.rser.2013.08.047

Nomenclature

T_C	working temperature of solar cell (Kelvin)
R_{SH}	shunt resistance
R_S	series resistance
N_S	series number of cells in a PV module
N_P	parallel number of modules for a PV array
I_{SC}	cell's short-circuit current at 25 °C and 1 kW/m^2
K_I	cell's short-circuit current temperature coefficient
T_{Ref}	cell's reference temperature
λ	solar insolation in kW/m^2
r	reflection coefficient of mirror
I_{RS}	cell's reverse saturation current at a reference temperature and solar radiation
E_g	band-gap energy of the semiconductor used in the cell
I_S	cell saturation or dark current
q	electron charge (1.6×10^{-19}C)
A	ideality factor
V_{OC}	open-circuit voltage
r_d	dynamic resistance
MPP	maximum power point
P_{MAX}	maximum power
CR	concentration ratio
FF	fill factor
η	efficiency
G_t	total in-plane solar radiation (W/m^2)
H_t	total in-plane solar insolation (kW h/m^2)
A_a	array area
R_{s0}	Series resistance of one solar cell
R_{sh0}	Shunt resistance of one solar cell

Subscripts

deg	degradation
PV	photovoltaic
soil	soiling
temp	temperature
STC	standard test condition

megawatts. Solar energy is effectively utilized in two ways, i.e., either by using it directly for heating or cooling of air and water without using an intermediate electric circuitry (i.e., solar thermal), or by converting it into electrical energy by using solar photovoltaic (PV) modules. Direct conversion of solar radiation into electrical energy is the most suitable way of utilizing solar energy. Among the various PV technologies, Si is one of the widely used semiconductors for the fabrication of solar cell. About 80% to 90% of PV cells manufactured worldwide are Si wafer based solar cells. The price of electricity generated from solar cell is quite high as compared with the conventional electricity price. Further cost reduction of the solar cell is possible by using thin c-Si wafers [2], thin film c-Si [3], Si in the form of ribbon [4,5], and concentrator Si solar cell [6,7]. In last decade price of silicon based solar module is reduced by a factor of 1/5 making it more relevant to develop low-concentration photovoltaic's using these cells.

Concentrator photovoltaic (CPV) technologies are usually classified according to its concentration ratio, i.e., low, medium and high concentration systems [8,9]. The major hindrance in medium and high concentration is as follows:

(A) The cell temperature increases with increase in concentration of light and being a semiconductor material it has a negative temperature coefficient of open-circuit voltage. As a result the solar cell loses its efficiency.
(B) Concentrating system uses direct sunlight, so they require an accurate sun tracking system. With the increase in concentration a high precision in tracking and optics is required [7].

Low concentration photovoltaic (LCPV) systems with a concentration ratio below 10 suns present following advantages:

A) LCPV systems can make use of conventional high performance silicon solar cells (made for 1 sun application [10])
B) LCPV systems are less demanding in terms of tracking accuracy as compared to high concentration systems [11]

Recently, there has been a renewed interest in the low concentration Si solar PV systems [12–16]. In this technology the commercial Si solar cell is used under the concentration of 2 suns to 10 suns. The improvement in performance is obtained by reducing the series resistance of the solar cell by using commercial techniques like electro-deposition of front metal contacts with Ag [3]. Many research groups across the globe have been working on concentration photovoltaic systems with innovative system designs, solar PV cell designs, cooling aspects, reflector geometry optimization, electrical characterization, non-uniformity in illumination and performance analysis [16–27]. A lot of work has been done in designing and analysis of the low concentration photovoltaic system (LCPV) [28–35]. An industrialization potential of silicon based concentrator photovoltaic system with an estimated cost of \$0.5/W$_p$ is reported by Castro et al. [17], where the group uses back contact solar cells under 100 suns. A detailed review of modeling in relation to low-concentration photovoltaic system is presented by Zahedi [28]. Li et al. have studied the performance of solar cell array based on a trough concentrating photovoltaic/thermal system [34]. Recently, Schuetz et al. [35] have reported design and construction of $\sim 7\times$ low-concentration CPV system based on compound parabolic concentrators. Recently our group has presented design, development and analysis of LCPV system [10,31,32]. The present work is an extension of the previously reported work, focusing particularly on the scalability of LCPV systems for commercial applications and its performance analysis.

2. Performance prediction model

2.1. Performance model for single module

A solar PV module is an integral part of the solar power generation system which is made-up of series connected solar

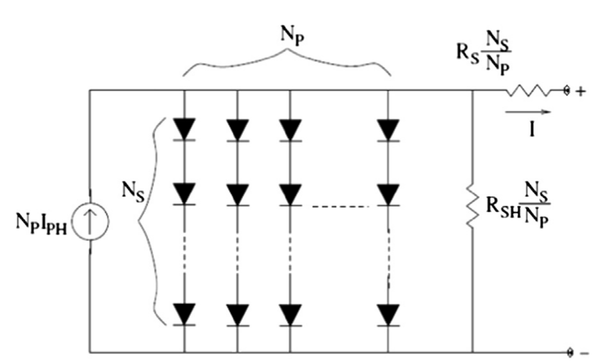


Fig. 1. The general model for LCPV module.

cells. Solar cell is basically a semiconductor *p*–*n* junction device which directly converts solar radiation into electricity through solar photovoltaic effect exhibited by the *p*–*n* junction. When a solar PV module is exposed to solar radiation, it shows non-linear current–voltage characteristics. The non-linear output current–voltage characteristic curve of a solar PV module is mainly influenced by the solar radiation and cell temperature. There exist many mathematical models for computer simulation, which describe the effect of solar radiation and cell temperature on output current–voltage characteristics of solar PV module [36–38].

A crystalline silicon wafer-based solar photovoltaic (PV) cell of size 156 mm × 156 mm typically produces around 3.8 W at a voltage of 560 mV. These cells are connected in series and/or parallel configuration in a module to produce desired power. The equivalent circuit of solar PV module, having N_P numbers of cells arranged in parallel and N_S number of cells arranged in series, is shown in Fig. 1.

The terminal equation for current and voltage of the solar PV array is mentioned below as described by many groups [39–42]:

$$I = N_P I_{PH} - N_P I_S\left[\exp\left(\frac{q\left(\frac{V}{N_S}+\frac{IR_S}{N_P}\right)}{k_B T_C A}\right)-1\right]-\left(\frac{N_P V}{N_S}+IR_S\right)/R_{SH} \tag{1}$$

Ideally in a solar PV module lower series resistance and very high shunt resistance is expected for higher power generation. A solar PV module mainly consists of three types of resistance: series resistance (R_S), shunt resistance (R_{SH}) and dynamic resistance (r_d). The series resistance, R_S can be determined by various illumination conditions such as dark, constant illumination and varying illumination and they yield different results [43]. Practically, R_S is determined by using two different illumination levels, the so-called two-curve method. Shunt resistance, R_{SH}, can be obtained from only one illuminated *I–V* curve, or single curve method. The output impedance of solar PV module, i.e., dynamic resistance is usually composed of the series resistance and shunt resistance at maximum power point (MPP).

In order to estimate the dynamic resistance which is defined as the negative reciprocal of dI/dV, Eq. (1) is differentiated with respect to V, i.e.,

$$\frac{dI}{dV} = -\frac{N_P}{N_S R_{SH}} - \frac{dI}{dV}\times\frac{R_S}{R_{SH}} - \frac{N_P I_S q}{kT_C A}\left[\frac{1}{N_S}+\frac{dI}{dV}\times\frac{R_S}{N_P}\right] \times\exp\left[\frac{q}{kT_C A}\times\left(\frac{V}{N_S}+\frac{IR_S}{N_P}\right)\right] \tag{2}$$

When the load is disconnected from the LCPV module and the output current (I) is equal to zero, Eq. (2) can be expressed by

$$\left.\frac{dI}{dV}\right|_{V=V_{OC}} = -\frac{N_P}{N_S R_{SH}} - \left.\frac{dI}{dV}\right|_{V=V_{OC}}\times\frac{R_S}{R_{SH}} - \frac{N_P I_S q}{kT_C A}\left[\frac{1}{N_S}+\left.\frac{dI}{dV}\right|_{V=V_{OC}}\times\frac{R_S}{N_P}\right] \times\exp\left[\frac{q}{kT_C A}\times\frac{V}{N_S}\right] \tag{3}$$

Therefore series resistance, R_S can be derived from Eq. (3)

$$R_S = \frac{R_{s0} N_P}{N_S} - \frac{kT_C A}{qI_S}\exp\left[-\frac{q}{kT_C A}\times\frac{V_{OC}}{N_S}\right] \tag{4}$$

For short-circuit condition the output voltage of LCPV module is zero so Eq. (2) is reduced to

$$\left.\frac{dI}{dV}\right|_{I=I_{SC}} = -\frac{N_P}{N_S R_{SH}} - \left.\frac{dI}{dV}\right|_{I=I_{SC}}\times\frac{R_S}{R_{SH}} - \frac{N_P I_S q}{kT_C A}\left[\frac{1}{N_S}+\left.\frac{dI}{dV}\right|_{I=I_{SC}}\times\frac{R_S}{N_P}\right] \times\exp\left[\frac{q}{kT_C A}\times\left(\frac{I_{SC}R_S}{N_P}\right)\right] \tag{5}$$

Therefore the shunt resistance, R_{SH} can be derived from Eq. (5):

$$R_{SH} = \frac{N_S}{N_P} R_{sh0} \tag{6}$$

Generally, for the solar PV modules $I_{PH} \gg I_S$, so in Eq. (1), the small diode and ground-leakage currents can be ignored under zero-terminal voltage. Therefore the short-circuit current is approximately equal to the photocurrent. The expression for I_{PH} is given by Eq. (7):

$$I_{PH} = [I_{SC} + K_I(T_C - T_{Ref})]\lambda \tag{7}$$

Where $\lambda = r \times CR \times$ Global Irradiation in W/m^2, r represents the reflection coefficient of mirrors.

The photocurrent (I_{PH}) mainly depends on the solar insolation and cell′s working temperature. The saturation current of a solar cell varies with the cell temperature, which is described by Eq. (8):

$$I_S = I_{RS}\left(\frac{T_C}{T_{Ref}}\right)^3 \exp\left[\frac{qE_g\left(\frac{1}{T_{Ref}}-\frac{1}{T_C}\right)}{k_B A}\right] \tag{8}$$

Reverse saturation current of the cell at reference temperature depends on the open-circuit voltage (V_{OC}) and can be approximately obtained by following equation as given by Tsai et al. [44]:

$$I_{RS} = I_{SC}/[\exp(qV_{OC}/N_S k_B A T_C) - 1] \tag{9}$$

The maximum power output of LCPV module is related to the I_{SC} and V_{OC} by following equation:

$$P_{MAX} = FF \times V_{OC} \times I_{SC} \tag{10}$$

The values of I_{SC}, V_{OC} and FF can be determined from the *I–V* characteristics obtained by Eq. (1).

The efficiency of the LCPV module in relation with the P_{MAX} is given by following equation

$$\eta = P_{MAX}/(A \times \lambda) \tag{11}$$

A is the aperture area of the PV module and λ is the incident solar radiation (W/m^2).

The characteristic parameters of LCPV module i.e., series resistance and the shunt resistance are dependent on the semiconductor fabrication process as well as the weather condition and can be calculated by Eqs. (4) and (6). Based on the theoretical model described above, the LCPV system is simulated using MATLAB/Simulink.

2.2. Model for LCPV power plant performance evaluation

The total daily ($E_{DC,d}$) and monthly ($E_{DC,m}$) energy generated by the LCPV system is given by Eqs. (12) and (13) [45],

$$E_{DC,d} = \sum_{t=1}^{t=24} E_{DC,t} \tag{12}$$

$$E_{DC,m} = \sum_{d=1}^{N} E_{DC,d} \tag{13}$$

where N is the number of days in the month. The instantaneous energy output could be obtained by measuring the energy generated by the LCPV system after the DC/DC converter.

The array yield (Y_A) is defined as the energy output from a PV array over a defined period (day, month or year) divided by its rated power [46] and is given by Eq. (14) as,

$$Y_A = \frac{E_{DC}}{P_{PV,rated}} \tag{14}$$

The daily array yield ($Y_{A,d}$) and monthly average daily array yield ($Y_{A,m}$) [47] are given by Eqs. (15) and (16) as follows:

$$Y_{A,d}=\frac{E_{DC,d}}{P_{PV,\text{rated}}} \tag{15}$$

$$Y_{A,m}=\frac{1}{N}\sum_{d=1}^{N} Y_{A,d} \tag{16}$$

The final yield is defined as the annual, monthly or daily net DC energy output of the system divided by the rated power of the installed PV array at standard test conditions (STC) of 1 kW/m^2 solar irradiance and 25 °C cell temperature. This is a representative figure that enables comparison of similar LCPV/PV systems in a specific geographic region. It is independent on the type of mounting, vertical on a façade or inclined on a roof and also on the location. The annual final yield is given by Eq. (17) as [48],

$$Y_{F,a}=\frac{E_{DC,a}}{P_{PV,\text{rated}}} \tag{17}$$

The daily final yield ($Y_{F,d}$) and the monthly average daily final yield ($Y_{F,m}$) is given by Eq. (18),

$$Y_{F,d}=\frac{E_{DC,d}}{P_{PV,\text{rated}}} \text{ and } Y_{F,m}=\frac{1}{N}\sum_{d=1}^{N} Y_{F,d} \tag{18}$$

The reference yield is the total in-plane solar insolation $H_t(\text{kW h}/m^2)$ divided by the array reference irradiance$(1\ \text{kW}/m^2)$. It is the number of peak sun-hours and is given by Eq. (19) [48]:

$$Y_R=\frac{H_t(\text{kW h}/m^2)}{1(\text{kW}/m^2)} \tag{19}$$

The performance ratio (PR) indicates the overall effect of losses on a LCPV array′s normal power output depending on array temperature and incomplete utilization of incident solar radiation and system component inefficiencies or failures. The PR of a LCPV system indicates how close it approaches the ideal performance during real operation and allows comparison of LCPV systems independent of location, tilt angle, orientation and their normal rated power capacity. The LCPV system efficiency is compared with the nominal efficiency of the photovoltaic generator under standard test conditions. Performance ratio is defined by Eq. (20) as follows [49,50]:

$$PR=\frac{\eta_{sys}}{\eta_{STC}}=\frac{E_{DC}}{G_t}\frac{G_{STC}}{P_{DC,STC}}=\frac{E_{DC}}{G_t\eta_{STC}} \tag{20}$$

where

$$\eta_{sys}=\frac{E_{DC}}{A_aG_t} \text{ and } \eta_{STC}=\frac{P_{DC,STC}}{A_aG_{STC}} \tag{21}$$

Performance ratio is also expressed by Eq. (22) [46,47,51]:

$$PR=\frac{Y_F}{Y_R}=\frac{E_{\text{real}}}{E_{\text{ideal}}}=\eta_{\text{deg}}\eta_{\text{tem}}\eta_{\text{soil}}\eta_{\text{inv}} \tag{22}$$

The capacity factor (CF) is a means to present the energy delivered by an electric power generating system. If the system delivers full rated power continuously, its CF would be unity. The capacity factor (CF) is defined as the ratio of the actual annual energy output to the amount of energy the LCPV system would generate if it is operated at full rated power ($P_{PV,\text{rated}}$) for 24 h per day for a year and is given by Eq. (23) [46]:

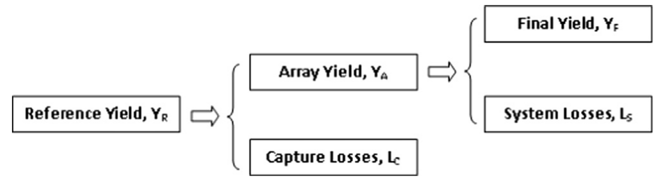


Fig. 2. Representation of relationships among normalized parameters.

$$CF=\frac{Y_{F,a}}{24\times 365}=\frac{E_{DC,a}}{P_{PV,\text{rated}}\times 8760}=\frac{H_t\times PR}{P_{PV,\text{rated}}\times 8760} \tag{23}$$

The CF for a grid connected LCPV system is also given by Eq. (24) [52]:

$$CF=\frac{\text{h/day of "peak sun"}}{24\ \ \text{h/day}} \tag{24}$$

Array capture losses (L_c) are due to the LCPV array losses and is given by Eq. (25) [46]:

$$L_c=Y_R-Y_A \tag{25}$$

System losses (L_s) are as a result of the inverter and is given by Eq. (26) [46]:

$$L_s=Y_A-Y_F \tag{26}$$

According to the above definitions the relationship among these normalized parameters is briefly shown in Fig. 2. One complete year is usually used in analyzing the energy performance of the LCPV system. In this article, the performance of 1 kW LCPV system (Fig. 3) with a concentration ratio of 3.3 sun is anticipated using real-time data of a sub-unit ($\approx$50 W_p) of LCPV system.

3. Development of a sub-unit of 1 kw LCPV system

A piecewise linear parabolic LCPV system is developed as shown in Fig. 4. The effective aperture area available using 6 mirrors is 1 m^2 and the effective receiver area is 0.11 m^2. In this LCPV system the reflecting mirrors can be added or removed so that effective aperture area can be changed and as a result concentration ratio can be varied. The receiver is made of a solar PV module fabricated by a string of thirty four silicon cell pieces (material: mono-crystalline silicon, size: 25 mm × 110 mm, efficiency $\approx$19%) cut from commercially available solar cell. The reason behind the selection of the specific size of the cells mentioned here is to solve the current handling problem of the solar cells under concentration. A typical solar cell of size 156 mm × 156 mm producing 3.8 W at a voltage of 560 mV would have a current handling capability of around 8 A. This cell, when used under 5 sun concentration may produce 40 A current by assuming a linear relationship between the current increment and concentration ratio (CR). But if the size of the cell is reduced to 1/5th of normal size, then the current generated under 5 sun concentration would be less than or equal to 8 A, and it will be easily handled without damaging the solar cell contacts.

The incident solar radiation is reflected by the piecewise linear parabolic trough concentrator (PLPTC) and concentrated in the focal plane having width of 110 mm. The receiver is mounted at the focal plane to intercept all the reflected radiation from PLPTC. The effective concentration is dependent on the

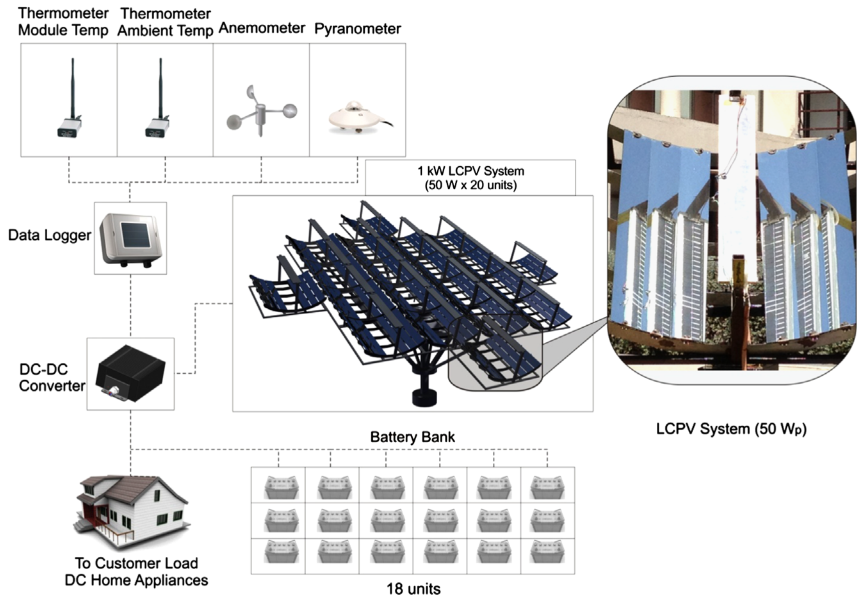


Fig. 3. Layout of 1 kW LCPV system for DC load applications.

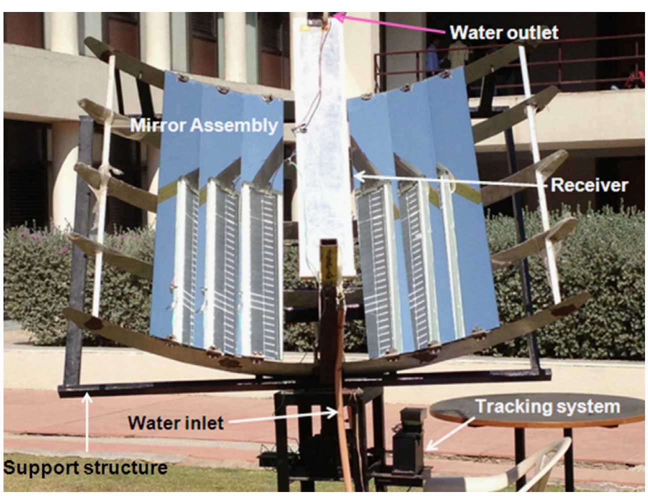


Fig. 4. The low-concentration photovoltaic system under actual test conditions.

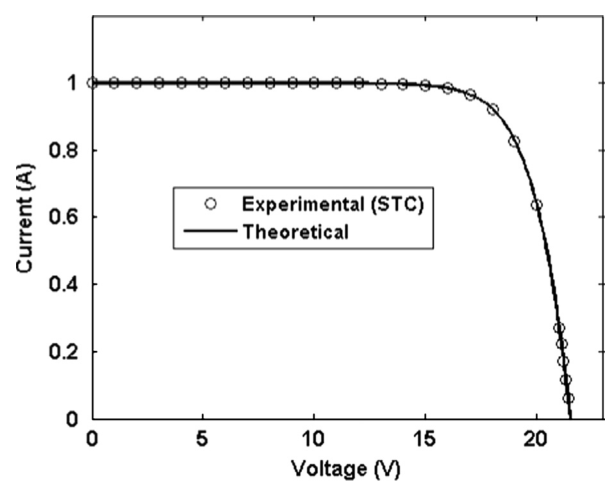


Fig. 5. Current–voltage characteristics of LCPV module under STC.

reflectivity of the mirrors used in PLPTC. In this case the reflectivity of the mirrors used is measured as ~77%. A microcontroller based one axis tracking system is developed for tracking the sun with a provision of manual tracking on the second axis.

The experiments were carried out in campus of School of Solar Energy located in Gandhinagar, India (Lat: 23.22°, Long: 72.68E) in the month of December and January (Year: 2012–2013). The module temperature was measured with digital thermometer having an accuracy of +0.1 °C on an hourly basis. Hourly solar radiation and ambient temperature were recorded at the weather station located in the University campus. The current and voltage are measured by varying load across the LCPV module under the ATC. The following parameters were measured hourly during experiments: ambient temperature, solar radiation, LCPV module temperature, load current, load voltage, short circuit current and open circuit voltage. During the experiment, the module temperature was maintained in the range of 32–38 °C by using continuous water flow behind LCPV module.

4. Validation and analysis of theoretical model

4.1. Validation and analysis of model under STC condition

A MATLAB/Simulink computer code is developed using mathematical model reported in Section 2 to simulate LCPV system. The data generated from the sub-unit of LCPV system (≈50 W) is used to validate the developed theoretical model under STC. The concentrated light is received by solar PV module which is placed at the focal plane of the PLPTC. To simulate electrical power generated from this PV module, computer program needs the value of series resistance, shunt resistance, energy band gap, and number of cells connected in series, number of strings connected parallel to each other, cell temperature, ambient temperature, short-circuit current of module, open-circuit voltage of module etc.

In this LCPV system a solar PV module manufactured at WAAREE Energies Pvt. Ltd. is used. The open-circuit voltage and short-circuit current of this module are measured as V_{OC}=21 V and I_{SC}=1 A, respectively, under AM1.5 spectrum at 25 °C. This module consists of only one string of thirty four cells of dimensions 25 mm × 110 mm connected in series. The current–

voltage output characteristic of generalized solar PV module under AM1.5 solar spectrum is shown in Fig. 5. The simulated current–voltage characteristic of developed solar PV module for the LCPV system is in accordance with the experimental current–voltage characteristics of this PV module. In the simulation short-circuit current, open-circuit voltage, series resistance and cell temperature measured under standard test conditions (STC) by manufacturer are taken as input parameters. The current–voltage characteristic generated from simulation program matches well with the experimental current–voltage characteristic.

4.2. Effect of concentration on static and dynamic parameters

The proposed model in Section 2 is used to estimate the *I–V* characteristics of the LCPV module. The static parameters (I_{SC}, V_{OC}, P_{MAX} and R_S) of the LCPV module are measured in ATC conditions as well as calculated by the proposed theoretical model. Fig. 6 presents the *I–V* curve of a LCPV system under the ATC. The test condition for one mirror is given by: solar radiation of 826 W/m^2 and module temperature of 31 °C. The maximum power at this condition was 10.23 W. The test condition for four mirrors is given by: solar radiation of 926 W/m^2 and module temperature of 39 °C. The maximum power at this condition was 36 W. The measured/calculated values of I_{SC}, V_{OC}, P_{MAX}, R_S and r_d with respect to solar radiation are listed in Tables 1 and 2. Generally, the output current of the solar PV modules increases with the radiation intensity. With an increase in the solar irradiance, the higher number of photons strikes the solar PV module which results in enhanced electron-hole pair generation and consequently higher photocurrent [53].

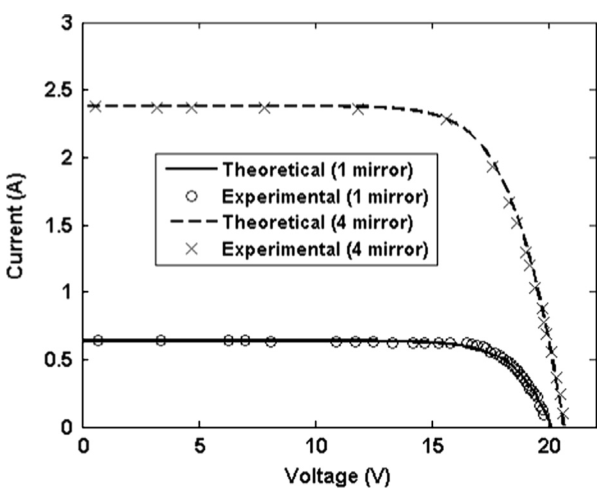


Fig. 6. Current–voltage characteristics of LCPV module under ATC.

Using our previous work [10,31,32], the dynamic resistance of LCPV module can be determined for a given photo-generated current–voltage characteristic curve. The values of the dynamic resistance at MPP are computed using the values of I_{SC} and R_S. The dynamic resistance of LCPV module is calculated using Eq. (2) and listed in Table 2. Approximate error between experimental and theoretical dynamic resistance of the LCPV modules is found within practically acceptable limits ($\approx$0.6%–2.8%). From obtained theoretical and observed experimental data as listed in Table 2, the series resistance, R_S shows a decreasing trend continuously with increase in the CR, which corresponds to increase in the intensity of illumination. Earlier researchers have also found the similar trend of variation of series resistance with increase in incident radiation [54,55]. The decrease in R_S can be attributed to increased conductivity of active layer with the increase in intensity of light, which further affects the dynamic resistance. The calculated and experimental values of dynamic resistance of the LCPV module show strong dependence on CR. The decrease in the dynamic resistance with increase in CR is attributed to the decreased R_S as shown by Eq. (2). By analysis of Eq. (2) it can be concluded that the dynamic resistance of LCPV module is dependent on the solar irradiance and solar PV module temperature. This is primarily caused by a logarithmic increase in V_{OC} and a linear increase in solar PV module photocurrent with increasing concentration. The dynamic resistance increases with the increase in temperature because of the increase in the series resistance [56–58].

The current–voltage characteristics shown in Fig. 6 and the data listed in Table 2 show the irradiation dependence of I_{SC}, V_{OC} and P_{MAX}. It is observed that the output power of LCPV module increases with the radiation intensity. Such an increase in output power is primarily caused by an increase in V_{OC} and also due to the linear increase in I_{SC}. The linear boost in I_{SC} is attributed to the increased minority carrier concentration due to increased incident light [53] with respect to the increasing number of mirrors. The LCPV module exhibits an extremely non-linear current–voltage behavior that varies continuously with change in solar radiation and module temperature. In this scenario, it is very important to explore the reliability of the LCPV system by the testing and

Table 1
The parameters used for simulation under 1 sun.

Module parameter	R_S (Ω)	E_g (eV)	N_S	N_P	A	T_c (K)	T_{ref} (K)	K (J/K)	K_I	Q (C)	I_{SC} (A)	I_{RS} (A)	V_{OC} (V)
For 1 sun	0.012	1.12	34	1	1.3	298	298	1.38×10^{-23}	0.65×10^{-3}	1.602×10^{-19}	0.259	0.86×10^{-12}	9.86

Table 2
Static and dynamic parameters of LCPV system under varying concentration.

Number of mirrors	Irradiance (W/m^2)	Experimental results					Theoretical estimation					Error, r_d (+ %)
		V_{OC} (V)	I_{SC} (A)	P_{MAX} (W)	R_S (Ω)	r_d (Ω)	V_{OC} (V)	I_{SC} (A)	P_{MAX} (W)	R_S (Ω)	r_d (Ω)	
1	826	19.8	0.64	10.00	2.56	87.04	20.1	0.64	9.82	2.58	87.72	0.8
2	852	20.2	1.16	17.86	1.68	57.12	20.2	1.16	17.71	1.67	56.78	0.6
3	870	20.4	1.60	24.53	1.29	43.86	20.4	1.60	24.56	1.28	43.52	0.8
4	926	20.6	2.38	35.60	1.03	35.02	20.6	2.38	36.19	1.00	34.00	2.8

analyzing the real-time data in outdoor conditions for the whole day. A series of experiments are conducted to examine the dynamic behavior of the LCPV module by considering finite series resistance and shunt resistance of the LCPV module.

4.3. Effect of LCPV module temperature on static and dynamic parameters

The effects of the cell temperature (T_C) on I–V curve of LCPV module is estimated from the proposed model as described in Section 2. As the device temperature increases, a small increase in short-circuit current is observed, however the open-circuit voltage rapidly decreases due to the exponential dependence of reverse saturation current on the temperature as given by Eq. (9) [53]. The changes in performance parameters, V_{OC}, FF, r_d and η with change in LCPV module temperature are listed in Table 3. The values of dynamic resistance at MPP are computed using the values of I_{SC} and R_S. The dynamic resistance of LCPV module is calculated using Eq. (2). Theoretical estimation shows decrease in open circuit voltage (V_{OC}) with the increase in T_C because as temperature increases the band gap of the intrinsic semiconductor shrinks. The increased temperature causes reduction in V_{OC} and increase in the photocurrent for a given irradiance because of high injection of electrons from valance band to conduction band of a semiconductor material [53]. Similar effect of temperature on V_{OC} is observed under actual test conditions and it is found that V_{OC} decreases from 21 to 20.6 V with temperature coefficient of voltage ≈ -0.061 V/K as shown in Table 3. From the observed result it is concluded that FF and η of LCPV module decreases as the LCPV module temperature increases. The decrease in FF and efficiency of solar PV module with module temperature is strongly dependent on the increase in series resistance of LCPV module. As a result of increased temperature, higher series resistance offers greater resistive power losses equivalent to I^2R_S in LCPV module and thus reduce its performance by reducing the FF and efficiency.

4.4. Validation and analysis of model under ATC conditions

The solar irradiance was recorded by the weather station on the test day as shown in Fig. 7. The module temperature was recorded using a digital thermometer during experiments and shown in Fig. 8. The peak solar intensity was observed as 943 W/m^2 at solar noon. On the experiment day the average wind speed was 1.5 m/s and the maximum wind speed was 3 m/s. The temperature of the inlet water was in the range of 24–25 °C.

The temperature of LCPV module has reached maximum at solar noon time (during 12:30 to 13:30 h). Module temperature is mainly affected by ambient temperature, DNI solar radiation, wind speed, coolant flow rate. During the morning hours the LCPV module temperature increases mainly due to increase in the solar radiation received by the parabolic trough collector and a similar trend is followed during evening hours which is in accordance with the variation in solar radiation as shown in Fig. 7.

The hourly output power trend and short-circuit current of LCPV module shown in Figs. 9 and 10 follows the hourly solar radiation shown in Fig. 7. The maximum power of ~38.5 W is observed during 12–13 h. The increase in power output of LCPV module is mainly dependent upon the solar irradiation, module temperature, wind speed, short-circuit current and open-circuit voltage. The wind velocity variation is responsible for a small disparity of +0.04 A in short-circuit current data during 13–14 h. The small variation in short-circuit current is extended to the

Table 3
Output electrical parameters of LCPV system under varying module temperature.

T_C (K)	Experimental results				Theoretical estimation				Error, η (+%)
	r_d (Ω)	V_{OC} (V)	FF (%)	η (%)	r_d (Ω)	V_{OC} (V)	FF (%)	η (%)	
305.6	32.4	21.0	81	15.4	32.4	21.1	80	15.5	0.6
307.5	33.8	20.9	80	15.1	33.8	21.0	78	15.0	0.7
312.1	35.6	20.6	77	14.4	35.6	20.7	77	14.4	0.0

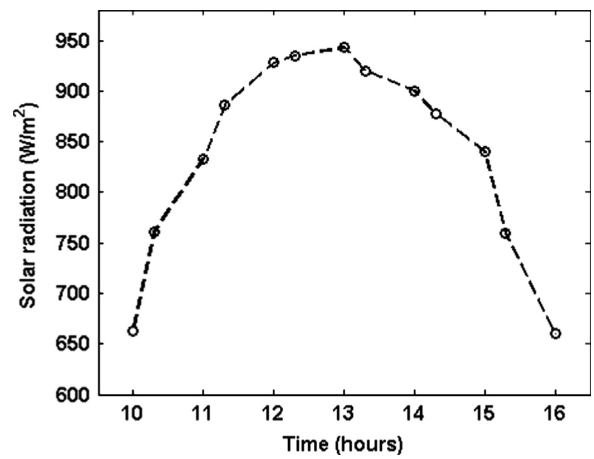


Fig. 7. Solar radiation with respect to day time.

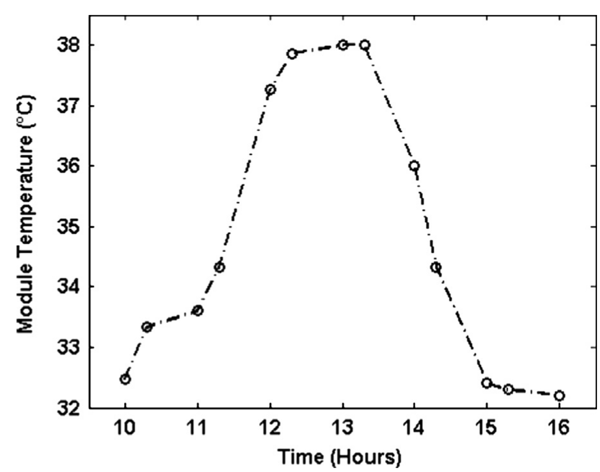


Fig. 8. Hourly LCPV module temperature variation with respect to day time.

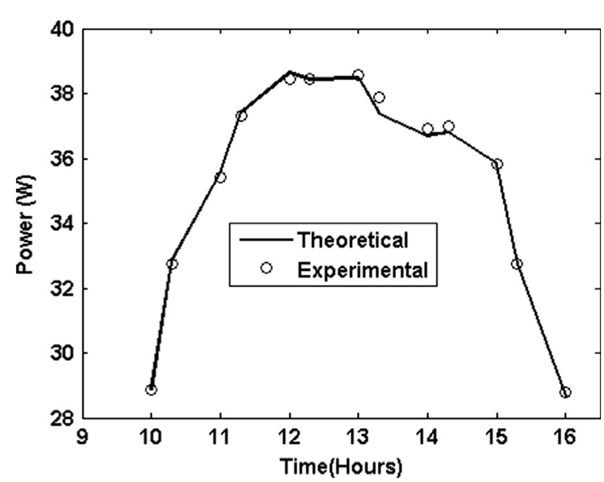


Fig. 9. Output power of LCPV system with respect to day time.

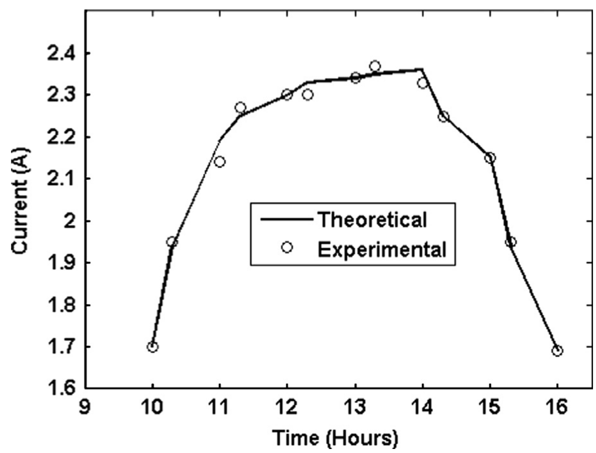


Fig. 10. Short-circuit current of LCPV system with respect to day time.

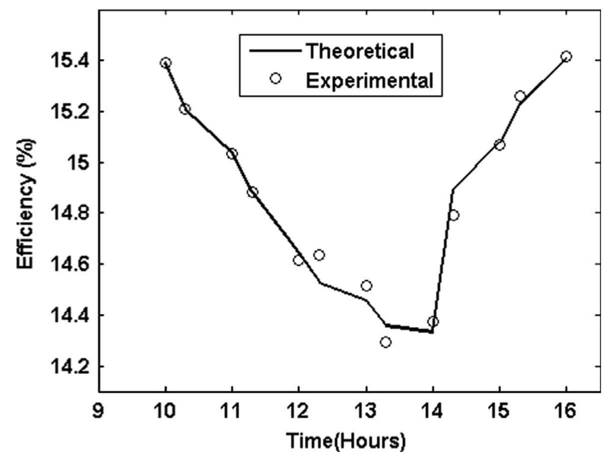


Fig. 12. Hourly variation of efficiency of LCPV module.

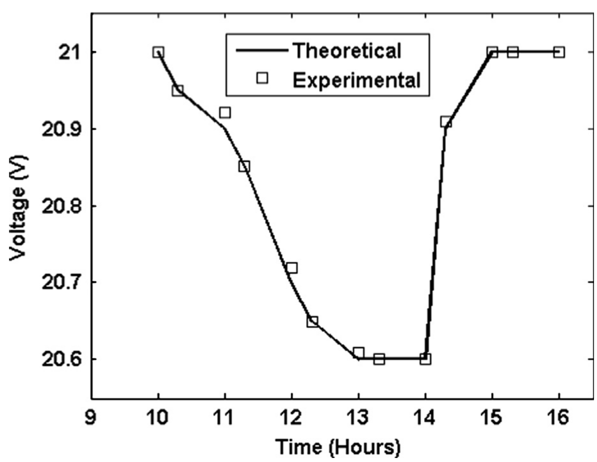


Fig. 11. Hourly variation of open-circuit voltage of LCPV module.

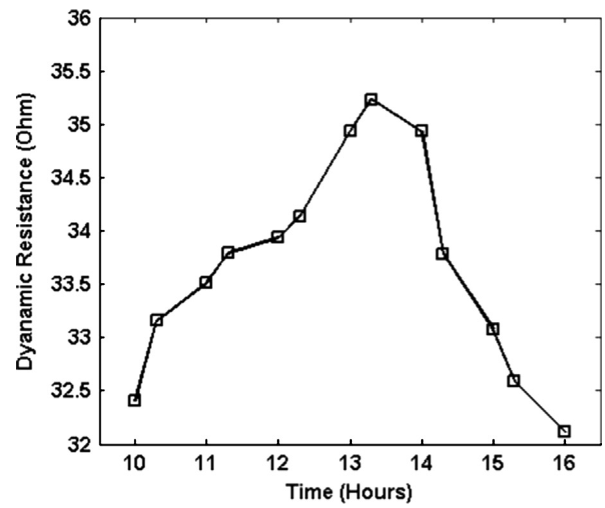


Fig. 13. Hourly variation of dynamic resistance of LCPV module with respect to day time.

output power fluctuation. This is mainly due to increased LCPV module temperature because of the influence of solar radiation and lowered wind speed during 13–14 h. The increased module temperature causes positive change in current and negative change in voltage. This results in power output decline from 38.5 to 36.5 W as observed in Fig. 9. It is observed that the open-circuit voltage and efficiency of LCPV module follows negative trend with respect to the change in module temperature as shown in Figs. 11 and 12, respectively. The maximum open-circuit voltage of 21 V and efficiency of ~15.4% is observed in morning at 10 h, which is due to least LCPV module temperature. The decrease in open-circuit voltage and efficiency of LCPV module with respect to time of the day is mainly due to increase in module temperature.

The dependence of dynamic resistance on LCPV module temperature is estimated using reported theoretical model in Section 2 at a constant solar radiation of 943 W/m^2 and shown in Fig. 13. The observed variation of dynamic resistance is attributed to the variation in LCPV module temperature as shown in Fig. 8. The dynamic resistance increases with increasing module temperature due to increase in series resistance as per Eq. (2). Existing literature also reports that series resistance increases with increase in module temperature [32,43]. From Eq. (2) it is evident that dynamic resistance strongly depends on series resistance which further depends on temperature at a given solar irradiation. This temperature dependence study indicates that the dynamic resistance has a positive coefficient of module temperature i.e., dr_d/dT given by 0.49 Ω/K. The estimated dependence of dynamic resistance on positive coefficient of temperature can play critical role in designing and development of maximum power point tracking (MPPT) systems.

5. Performance evaluation of 1 kW LCPV system

The monthly average in-plane solar radiation on the LCPV system is taken from weather station installed in University campus for the period of January to December′2012 as shown in Fig. 14. The monthly average solar radiation varied from 600 W/m^2 in August to 1100 W/m^2 in February. The number of rainy days and average wind speed over the monitoring period is shown in Figs. 15 and 16, respectively. The average wind speed varied between 0.6 m/s in February and 1.15 m/s in August. The average monthly energy generated by the LCPV plant is calculated by using the Eqs. (12) and (13). Fig. 17 shows that the monthly total energy generated by the LCPV system varied from a lower value of 95 kW h/kW$_p$ in the month of August to a maximum value of 182 kW h/kW$_p$ in the month of March. The gross electricity generation per year would be 1747 kW h/kW$_p$ with a monthly average of 145 kW h/kW$_p$. The production is accentuated when the radiation level is high which indicates that LCPV system outperform under high levels of insolation. However the response to diffuse radiation was similar and low level of solar radiation produce insignificant difference in production. Ambient temperature is another parameter which influences the LCPV energy

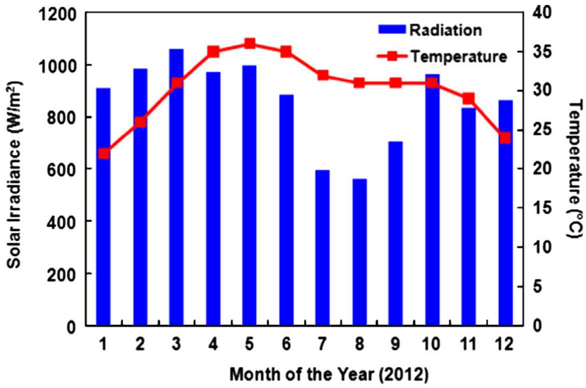


Fig. 14. Average monthly solar radiation and ambient temperature over the monitored period.

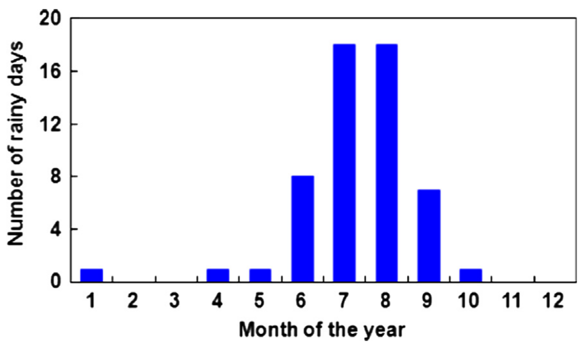


Fig. 15. Number of rainy days over the monitored period.

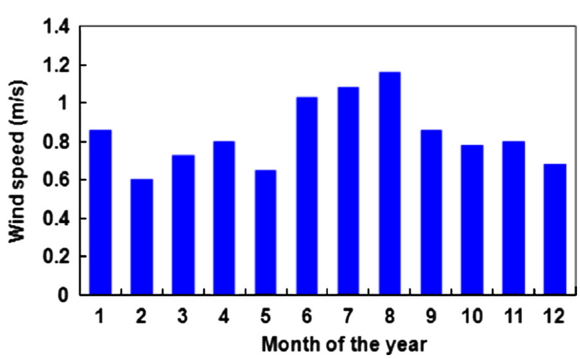


Fig. 16. Variation of wind speed over the monitored period.

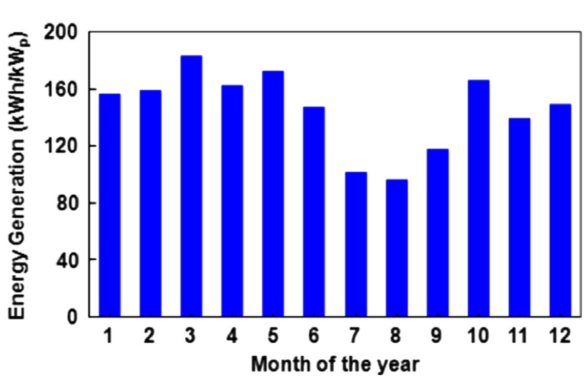


Fig. 17. Monthly total energy generated over the monitored period.

production. A seasonal classification of results allows us to relate the effect of ambient temperature and wind speed on performance of LCPV system. The greatest differences in energy production are observed in summers when the hours of sunshine are higher whereas in the colder months the difference in energy production is insignificant.

The most appropriate performance indicators which may be used to define overall LCPV system performance with respect to energy production, solar resources and overall effect of system losses are: final yield, reference yield, performance ratio (PR), system loss and capture loss. The final yield normalizes the energy produced with respect to system size. Consequently it is a convenient way to compare the LCPV systems with different sizes. It is expressed in hours/day. The reference yield represents the number of peak sun hours. It is a function of location, orientation and inclination of LCPV array. The final yield, reference yield and array yield is calculated using Eqs. (17)–(19). The summary of the normalized performance parameters is presented in Figs. 18–20. Fig. 18 indicates that the monthly final yield fluctuate greatly from a minimum value of 1.5 h/day in August to a peak of 5.5 h/day in March with an average of 3.76 h/d.

The most useful parameter is so called PR, which is a dimensionless quantity that indicates the overall effect of losses (due to converter inefficiency, cell temperature, losses in wiring, protection diodes, partial shading and module mismatch) on the rated output. The PR is defined as the ratio of DC energy delivered to the load to the energy production of an ideal lossless LCPV system with 25 °C cell temperature at 1000 W/m^2. Performance ratio value is important for identifying the occurrence of problems due to different system component failure; nevertheless it cannot identify the cause. For this reason, other interesting parameters associated with the PR can be used to distinguish between losses due to photovoltaic generator and losses associated with the DC–DC converters such as capture losses and system losses. Fig. 19

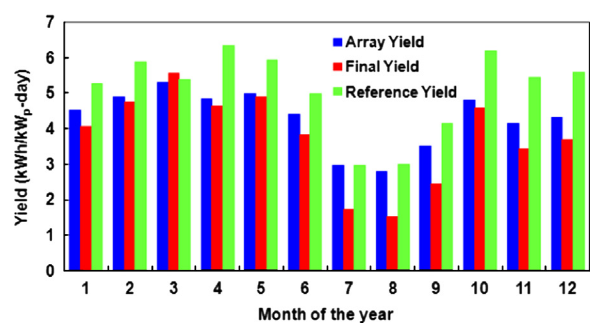


Fig. 18. Monthly average daily PV system's array yield, final yield and reference yield.

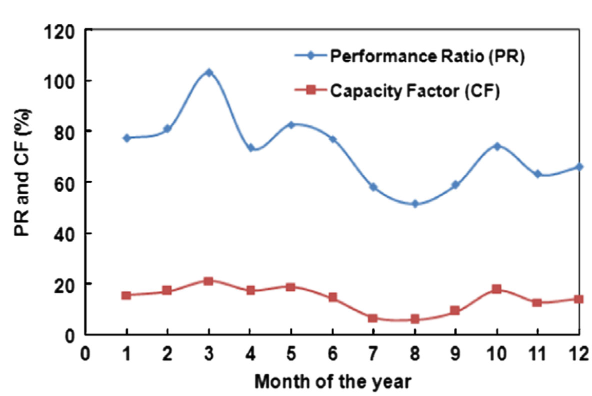


Fig. 19. Monthly average PR and CF of LCPV system.

represents the monthly average PR and capacity factor (CF). The performance ratio of the LCPV plant ranges from 0.51 to 1.02 for the studied LCPV system. The observed trend of PR shown in Fig. 19 follows the monthly radiation trend as shown in Fig. 14. A non-linear behavior of PR is observed due the non-linear current–voltage characteristics of LCPV modules which is discussed in Section 4.

During the year 2012, the operation of LCPV system generates about 1747 kW h. The normalized parameters, Y_F, L_S and L_C are shown for each month of 2012 in Fig. 20. The system losses are due to the losses in DC–DC conversion. The capture losses are due to LCPV array losses. The annual final yield is 74.7%, capture losses are 14.7% and system losses are 10.6% of the total energy balance of the LCPV power plant. In March 2012, the energy generation was largest (182 kW h), the final yield was 93.9%, capture losses were 1.7% and system losses were 4.4%. But in August 2012, the energy harnessing was least (95.7 kW h), the final yield was 51.2%, capture losses were 6.7% and system losses were 42.1%. The LCPV system has low capture losses as compared to the flat panel PV systems. This is mainly due to following reasons:

(a) The accumulation of thermal energy in the interior of flat photovoltaic (PV) modules as a consequence of continuous solar irradiation causes a difference between the junction temperature of the PV modules and the ambient temperature, which leads to a serious deterioration in the performance of the PV modules [45]. In case of LCPV systems the temperature difference between junction and ambient remains low due to continuous water flow at the backside of the LCPV modules which leads to maximum utilization efficiency of LCPV modules. This low temperature difference between junction and ambient is essentially responsible for low capture losses in LCPV systems.

(b) The second major factor which influences the capture losses is the hindrance in receiving sufficient illumination by the solar PV modules. This is mainly due to shading, inclination angle and the change in sun position during daytime with respect to the fixed flat PV system. This problem is overcome in an LCPV system by employing a low cost one-axis tracking system, which results in an increased solar energy harvesting (≈ 25%). This mechanism further reduces capture losses in an LCPV system.

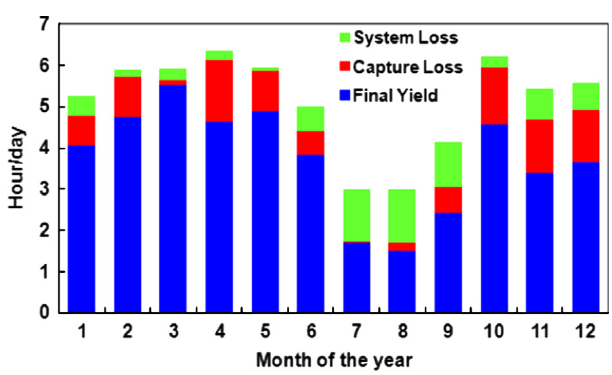


Fig. 20. Monthly performance of LCPV system.

The overall decrease in capture losses directly influences the final yield of the power plant. A comparison table of different existing solar PV power plants from different locations is given in Table 4. This comparison shows that the LCPV power plant may result in better final yield compared with flat panel PV systems. This type of system is more suitable for hot climatic conditions where it gives electrical energy (with a conversion efficiency of ≈ 10%) along with the hot water for various applications (with a conversion efficiency of ≈ 20%).

6. Economical analysis of LCPV system

An established method based on net present value (NPV), that allows analyzing the economic aspects of any engineering system, is used for the economic analysis of developed LCPV system of 1 kW_P. This method allows accounting for the present value of annual capital expenditures and savings during the lifetime of the system. Net present value (NPV) includes sum of all the current values (costs are shown negative, and net savings are shown as positive). The feasibility of the engineering system is dependent on the NPV value, which must be positive for acceptance of the project. The formulas for calculating NPV and corresponding factor are given as [62]:

$$NPV = \sum_{i=1}^{n} (B-C)_i \tag{27}$$

$$a = \frac{1}{(1+i)^p} \tag{28}$$

Table 4
Performance parameter comparison for various PV systems.

Location	PV type	Final yield (h/d)	Module efficiency (%)	System efficiency (%)	Performance ratio (%)	Reference
Málaga, Spain	Poly-Si	3.7	10.3	8.0	64.5	[59]
Jaén, Spain	Poly-Si	2.4	8.9	7.8	62.7	[60]
Ballymena, Ireland	Mono-Si	1.7	10.0	9.0	62.0	[48]
Castile & Leon, Spain	Mono-Si	1.4–4.8	13.7	12.2	69.8	[61]
Gandhinagar, India	Mono-Si	1.5–5.5	15.5	10.0	72.0	Present study

Table 5
Cost of various components of LCPV system (≈ 1 kW_P) to find initial investment cost (numbers provided here are in accordance with the current market price)[a].

Components	Module	BOS				
		Battery	Charge controller	Support structure	Tracker	Cabling
Cost (in US$)	206	800	48	320	590	120
Total initial investment cost (in US$)						2084

[a] The price is based on market survey, which may vary depending on specific location or company.

Table 6
Economical analysis of LCPV system.

Period (year)	0	1	2	3	4	5	6	7	8
Initial investment cost	−2084								
Benefits**		290.43	290.43	290.43	290.43	290.43	290.43	290.43	290.43
O & M cost***		−2.18	−2.30	−2.43	−2.57	−2.72	−2.88	−3.04	−3.21
Discount rate	0.01	0.01	0.01	0.01	0.01	0.01	0.01	0.01	0.01
Net cash flow		288.25	288.13	287.995	287.86	287.71	287.55	287.39	287.21
a	0.99	0.99	0.98	0.97	0.96	0.95	0.94	0.93	0.92
Discounted net cash flow		285.39	282.45	279.53	276.62	273.74	270.89	268.05	265.24
NPV		−1798.6	−1516.2	−1236.6	−960	−686.26	−415.37	−147.32	117.92

** Benefits are based on the tariff policy of Gujarat Electricity Regulatory Commission released for projects commissioned in 2012 [63].
*** Escalation in operating cost is taken as 5.72% annually [63].

where "a" represents net present value factor, "B" represents gain, "p" represents the period and "i" represents discount rate in the equation given above.

In order to calculate NPV, it is important to find initial investment cost which includes module cost and balance of systems (BOS) cost. The components of BOS include battery storage, charge controllers, support structure, tracking system and transmission cables. Cost of all these components is listed in Table 5. Using the initial investment cost and the formula outlined in Eqs. (27) and (28), the NPV is calculated (Table 6). Operation and maintenance (O & M) cost is taken as 0.75% of the total investment cost with escalation in operating cost as 5.72% per annum [63]. The feasibility of this project is demonstrated by a positive value of NPV obtained within 8 years.

7. Conclusions

In this study real-time performance analysis of commercially available crystalline silicon solar cell based LCPV system is presented. The experiments based on LCPV system were performed to investigate the feasibility of LCPV power plants. Under ATC, the open-circuit voltage, V_{OC} found decreasing with temperature coefficient of voltage ≈ -0.061 V/K. The dynamic resistance has a positive coefficient of module temperature i.e., dr_d/dT given by 0.49 Ω/K. The study reveals that the LCPV power plant has low capture losses compared to flat panel PV plant. The LCPV power plant has produced a better final yield compared with flat panel PV systems. This type of system is more suitable for hot climatic conditions where it gives electrical energy (with a conversion efficiency of $\approx$10%) along with the hot water for various applications.

Acknowledgements

The authors acknowledge the financial support provided by Gujarat Energy Development Agency (GEDA) to develop CPV system by grant number: GEDA\EC:REC\March-2010/3/9174. The authors also acknowledge WAAREE Energies Pvt. Ltd., India and Neety Euro-Asia Solar Energy, India for providing technical help for this study. The authors acknowledge Prof. Indrajit Mukhopadhyay for his continuous guidance.

References

[1] ⟨http://reneweconomy.com.au/2013/the-top-solar-countries-past-present-and-future-96405⟩ (accessed on February 11′ 2013).
[2] Chaudhari VA, Solanki CS. From 1 sun to 10 suns c-Si cells by optimizing metal grid, metal resistance, and junction depth. International Journal of Photoenergy 2009. http://dx.doi.org/10.1155/2009/827402.
[3] Solanki CS. Solar photovoltaics: fundamental, technologies and applications. 2nd ed. India: Prentice Hall; 2011.
[4] Schwirtlich IA. EFG ribbon technology, in high-efficient low-cost photovoltaics, Springer series in optical sciences. Berlin, Germany: Springer; 57–64.
[5] Pivac B, Borjanovi V, Kovacevi I, Evtody BN, Katz EA. Comparative studies of EFG poly-Si grown by different procedures. Solar Energy Materials and Solar Cells 2002;72:165–71.
[6] PA Basore. CSG-1: manufacturing a new polycrystalline silicon PV technology. In: Proceedings of the 4th IEEE world conference on photovoltaic energy conversion (WCPEC′07)2; 2007: p. 2089–2093.
[7] Cuevas A, Sinton RA, Midkiff NE, Swanson RM. Twenty-six-percent efficient point-junction concentrator solar cells with a front metal grid. Electron Device Letters 1990;11(1):6–8.
[8] Y Tripanagnostopoulos, M Souliotis, S Tselepis, V Dimitriou, Th Makris. Design and performance aspects for low concentration photovoltaics, 20th EUPVSEC, 6–10, Barcelona, Spain; 2005.
[9] Luque A, Andreev V. Concentrator photovoltaics. 1st ed. Berlin, Heidelberg, New York: Springer; 2007 (Chapter: 1 and 6).).
[10] Tripathi B, Yadav P, Lokhande M, Kumar M. Feasibility study of commercial silicon solar PV module based low concentration photovoltaic system. International Journal of Electrical and Electronics Engineering Research 2012;2(3):84–93.
[11] S Kurtz. Opportunities and challenges for development of a mature concentrating photovoltaic power industry, Technical report, NREL/TP-520- 43208; 2009).
[12] Cotana F, Rossi F, Nicolini A. Evaluation and optimization of an innovative low-cost photovoltaic solar concentrator. International Journal of Photoenergy 2011;2011:1–10 (Article ID 843209).
[13] Baig H, Sarmah N, Heasman KC, Mallick TK. Numerical modelling and experimental validation of a low concentrating photovoltaic system. Solar Energy Materials and Solar Cells 2013;113:201–19.
[14] Baig H, Heasman KC, Mallick TK. Non-uniform illumination in concentrating solar cells. Renewable and Sustainable Energy Reviews 2012;16:5890–909.
[15] Gajbert H, Hall M, Karlsson B. Optimisation of reflector and module geometries for stationary, low-concentrating, façade-integrated photovoltaic systems. Solar Energy Materials and Solar Cells 2007;91:1788–99.
[16] Grasso G, Righetti A, Ubaldi MC, Morichetti F, Pietralunga SM. Competitiveness of stationary planar low concentration photovoltaic modules using silicon cells: a focus on concentrating optics. Solar Energy 2012;86:1725–32.
[17] Liu CY, Lai CC, Liao JH, Cheng LC, Liu HH, Chang CC, et al. Nitride-based concentrator solar cells grown on Si substrates. Solar Energy Materials and Solar Cells 2013;117:54–8.
[18] Abu-Bakar SH, Muhammad-Sukki F, Ramirez-Iniguez R, Mallick TK, Mclennan C, Munir AB, et al. Is renewable heat incentive the future? Renewable and Sustainable Energy Reviews 2013;26:365–78.
[19] Al-Amri F, Mallick TK. Alleviating operating temperature of concentration solar cell by air active cooling and surface radiation. Applied Thermal Engineering 2013;59:348–54.
[20] Micheli L, Sarmah N, Luo X, Reddy KS, Mallick TK. Opportunities and challenges in micro- and nano-technologies for concentrating photovoltaic cooling: a review. Renewable and Sustainable Energy Reviews 2013;20:595–610.
[21] Or AB, Appelbaum J. Performance analysis of concentrator photovoltaic dense-arrays under non-uniform irradiance. Solar Energy Materials and Solar Cells 2013;117:110–9.
[22] Kim JM, Dutta PS. Optical efficiency–concentration ratio trade-off for a flat panel photovoltaic system with diffuser type concentrator. Solar Energy Materials and Solar Cells 2012;103:35–40.
[23] Hornung T, Steiner M, Nitz P. Estimation of the influence of Fresnel lens temperature on energy generation of a concentrator photovoltaic system. Solar Energy Materials and Solar Cells 2012;99:333–8.
[24] Rodrigo P, Fernández EF, Almonacid F, Pérez-Higueras PJ. Models for the electrical characterization of high concentration photovoltaic cells and modules: a review. Renewable and Sustainable Energy Reviews 2013;26:752–60.
[25] Chong K-K, Lau S-L, Yew T-K, Tan P C-L. Design and development in optics of concentrator photovoltaic system. Renewable and Sustainable Energy Reviews 2013;19:598–612.
[26] Du B, Hu E, Kolhe M. Performance analysis of water cooled concentrated photovoltaic (CPV) system. Renewable and Sustainable Energy Reviews 2012;16:6732–6.
[27] Gómez-Gil FJ, Wang X, Barnett A. Energy production of photovoltaic systems: fixed, tracking, and concentrating. Renewable and Sustainable Energy Reviews 2012;16:306–13.

[28] Zahedi A. Review of modelling details in relation to low-concentration solar concentrating photovoltaic. Renewable and Sustainable Energy Reviews 2011;15:1609–14.
[29] G Sala, I Anton, J Monedero, P Valera, MP Friend, M Cendagorta, et al. The Euclides-thermie concentrator power plant in continuous operation. In: Proceedings of the 17th EUPVSEC, Munich, Germany; 2001. p. 488–491.
[30] Reis F, Brito MC, Corregidor V, Wemans J, Sorasio G. Modeling the performance of low concentration photovoltaic systems. Solar Energy Materials and Solar Cells 2010;94:1222–6.
[31] Yadav P, Tripathi B, Lokhande M, Kumar M. Effect of temperature and concentration on commercial silicon module based low-concentration photovoltaic (LCPV) system. AIP Journal of Renewable and Sustainable Energy 2013;5 (013113-1-10).
[32] Yadav P, Tripathi B, Lokhande M, Kumar M. Estimation of steady state and dynamic parameters of low concentration photovoltaic system. Solar Energy Materials and Solar Cells 2013;112:65–72.
[33] Castro M, Anton I, Sala G. Pilot production of concentrator silicon solar cells: approaching industrialization. Solar Energy Materials and Solar Cells 2008;92:1697–705.
[34] Li M, Ji X, Li G, Wei S, Li Y, Shi F. Performance study of solar cell array based on a trough concentrating photovoltaic/thermal system. Applied Energy 2011;88:3218–27.
[35] Schuetz MA, Shell KA, Brown SA, Reinbolt GS, French RH, Davis RJ. Design and construction of a $\sim 7\times$ low-concentration photovoltaic system based on compound parabolic concentrators. IEEE Journal of Photovoltaics 2012. http://dx.doi.org/10.1109/JPHOTOV.2012.2186-283.
[36] Kerr MJ, Cuevas A. Generalized analysis of the illumination intensity vs. open-circuit voltage of PV modules. Solar Energy 2003;76:263–7.
[37] Radziemska E, Klugmann E. Thermally-affected parameters of the current–voltage characteristics of silicon photocell. Energy Conversion and Management 2002;43:1889–900.
[38] van Dyk EE, Meyer EL, Leitch AWR, Scott BJ. Temperature-dependent of performance of crystalline silicon photovoltaic modules. South African Journal of Science 2000;96(4):198–200.
[39] Veerachary M, Senjyu T, Uezato K. Voltage-based maximum power point tracking control of PV system. IEEE Transactions on Aerospace and Electronic Systems 2002;38(1):262–70.
[40] Veerachary M, Shinoy KS. V2-based power tracking for nonlinear PV sources. IEEE Proceedings—Electric Power Applications 2005;152(5):1263–70.
[41] Kim IS, Youn MJ. Variable-structure observer for solar array current estimation in a photovoltaic power-generation system. IEEE Proceedings—Electric Power Applications 2005;152(4):953–9.
[42] Kim IS, Kim MB, Youn MJ. New maximum power point tracker using sliding-mode observer for estimation of solar array current in the grid-connected photovoltaic system. IEEE Transaction on Industrial Electronics 2006;53 (4):1027–35.
[43] Thongpron J, Kirtikara K, Jivicate C. A method for the determination of dynamic resistance of photovoltaic modules under illumination,. Solar Energy Materials and Solar Cells 2006;90(18-19):3078–84.
[44] HL Tsai, CS Tu, YJ Su. Development of generalized photovoltaic model using MATLAB/Simulink. In: Proceedings of the world congress on engineering and computer science, October 22–24, San Francisco, USA; 2008.
[45] Ayompe LM, Duffy A, McCormack SJ, Conlon M. Measured performance of a 1.72 kW rooftop grid connected photovoltaic system in Ireland. Energy Conversion and Management 2011;52:816–25.
[46] Kymakis E, Kalykakis S, Papazoglou TM. Performance analysis of a grid connected photovoltaic park on the island of Crete. Energy Conversion and Management 2009;50(3):433–8.
[47] Photovoltaic Power Systems Programme, Cost and performance trends in grid-connected photovoltaic systems and case studies. IEA-PVPS T2-06; 2007.
[48] Mondol JD, Yohanis Y, Smyth M, Norton B. Long term performance analysis of a grid connected photovoltaic system in Northern Ireland. Energy Conversion and Management 2006;47(18–19):2925–47.
[49] H Nakagami, O Ishihara, K Sakai, A Tanaka. Performance of residential PV system under actual field conditions in western part of Japan. In: International solar energy conference, Hawaii, USA, ISEC2003-44228; 2003. p. 491–497.
[50] Eicker U. Solar technologies for buildings. England: John Wiley and Sons; 2003.
[51] The German Solar Energy Society, planning and installing photovoltaic systems: a guide for installers, architects and engineers, James and James, UK; 2006.
[52] Masters GM. Renewable and efficient electric power systems. New Jersey: John Wiley and Sons; 2004.
[53] Sze SM. Physics of semiconductor devices. 2nd ed. New York: Wiley; 1981.
[54] Arora JD, Verma AV, Bhatnagar M. Variation of series resistance with temperature and illumination level in diffused junction poly- and single-crystalline silicon solar cells. Journal of Materials Science Letters 1986;5 (12):1210–2.
[55] Khan F, Singh SN, Husain M. Effect of illumination intensity on cell parameters of a silicon solar cell. Solar Energy Materials and Solar Cells 2010;94:1473–6.
[56] Bose BK, Szczesny PM, Steigerwald RL. Microcomputer control of a residential photovoltaic power conditioning system. IEEE Transactions on Industry Applications IA-21 1985:1182–91.
[57] Zhou W, Yang H, Fang Z. A novel model for photovoltaic array performance prediction. Applied Energy 2007;84:1187–98.
[58] Pysch D, Mette A, Glunz SW. A review and comparison of different methods to determine the series resistance of solar cells. Solar Energy Materials and Solar Cells 2007;91:1698–706.
[59] Sidrach-de-Cardona M, López LM. Performance analysis of a grid-connected photovoltaic system. Energy 1999;24(2):93–102.
[60] Drif M, Pérez PJ, Aguilera J, Almonacid G, Gomez P, de la Casa J, et al. Univer project. A grid connected photovoltaic system of 200 kW_P at Jaén University. Overview and performance analysis. Solar Energy Materials and Solar Cells 2007;91(8):670–83.
[61] Miguel AD, Bilbao J, Cazorro JRS, Martin C. Performance analysis of a grid-connected PV system in a rural site in the northwest of Spain. World renewable energy congress VII, Cologne, Germany 2002.
[62] Kandilli C. Performance analysis of a novel concentrating photovoltaic combined system. Energy Conversion and Management 2013;67:186–96.
[63] ⟨http://www.gercin.org/renewablepdf/Solar%20Tariff%20Order%201%20of%202012.pdf⟩ (accessed on 22–07–2013).